NUCLEAR THEORY, Vol. 39 (2022)
eds. M. Gaidarov, N. Minkov, Heron Press, Sofia

A Systematic Study of Nuclear Stopping and Various Observables that Reflects the Degree of Thermalization

Rajat Rana, **Garima**, **Sakshi Gautam**, **Rajeev K. Puri**

Department of Physics, Panjab University, Chandigarh 160014, India

Abstract.

We performed a systematic study of various observables of nuclear stopping i.e. energy-based isotropy ratio (R_E), momentum-based isotropy ratio (R_p), *vartl*, for central collisions of various reactions, i.e. ^{40}Ca+^{40}Ca, ^{58}Ni+^{58}Ni, ^{129,120}Xe+^{124}Sn and, ^{197}Au+^{197}Au as energy dependence for soft momentum dependent equation of state with the help of Isospin-dependent Quantum Molecular Dynamics (IQMD) model. A confrontation of our calculation with experimental measurements of various nuclear stopping observables reveals that 20% in-medium nucleon-nucleon cross-section reduction for the soft momentum-dependent equation of state is apt to study the nuclear stopping observables. Such a conclusion reaches more assuredly by using the isospin tracing method and compared the experimental results with our calculations for collisions of different combinations reactions of ^{96}Zr+^{96}Ru and ^{96}Ru+^{96}Zr nuclei. Therefore, the comparison of dynamics model calculations with available measurements on isospin mixing also showed that in-medium NN cross-section reduction of 20% reproduces experimental data on nuclear stopping reasonably well.

1 Introduction

Heavy ion collisions provide an opportunity to produce a large volume of excited nuclear matter with high density and excitation as well as high temperature in a controlled manner [1]. It is worth mentioning that one of the goals of the heavy ion collisions (HICs) at intermediate energy is to learn about the fundamental properties of hot and dense nuclear matter under extreme conditions, namely the nuclear equation of state (EOS) [2]. The final products of such collisions are also useful in exploring some of the astrophysical phenomena such as the explosion mechanism of supernovas and formation of a neutron stars [3]. The transport models are required where one-body dissipation and two-body dissipation creates a link between the EOS extracted from the heavy ion collisions and various experimental observations [4]. In earlier decades, to extract the information about EOS by comparing the experimental data with various hydrodynamical approaches based on local equilibration postulate [2].

One of the key observables which provide information about nuclear EOS is nuclear stopping in heavy ion collisions which is previously studied with the help of rapidity distribution [5] and asymmetry of nucleon momentum distribution [6]. In previous studies, it was pointed out that nuclear stopping at intermediate energy is determined by both the mean-field and in-medium nucleon-nucleon cross-section [7]. Nuclear stopping is an ability of nuclear matter as a result of which the incoming longitudinal energy of projectile and target is converted into transverse degrees of freedom which ultimately slows down the incoming nucleons. Since the nuclear stopping is transverse as well as longitudinal in the direction so it is not suitable to use any vector variable such as transverse energy [8]. Therefore, to quantify the nuclear stopping power we use scalar quantities, like the energy-based isotropy ratio ($\mathbf{R}_E$) [8] and momentum-based isotropy ratio (R_P) [8], *vartl* [9] etc.

It is one of the helpful ingredients in extracting the information about EOS and nucleon-nucleon cross-sections like other observables which is collective flow but the information about transverse/elliptic flow shows its dual sensitivity towards symmetry energy as well as NN cross-section [10] while nuclear stopping is independent of symmetry energy [11] and therefore, helpful to provide information about in-medium NN cross-section. In a study by the INDRA Collaboration [8] using the Indra 4π array, it was found that nuclear stopping data provide a new opportunity to investigate the in-medium NN cross-section by comparing it with a transport model in HICs from tens of MeV/nucleon to thousands of MeV/nucleon and wonder to see the effect of in-medium NN cross-section. Several studies are there which predicted the stiffness of the equation of state of isospin symmetric nuclear matter [12] but we have a limited number of studies to extract the information for the in-medium NN cross-section. In the Fermi energy range, there is an interplay between two modes of dissipation i.e. one body dissipation and two body dissipation. In the energy range below Fermi energy, the one-body dissipation modes are predominantly proposed through the study of fusion cross-sections [13]. On contrary, above Fermi energy, the two-body dissipation mode is predominant which is mainly governed by NN collisions. These studies supported the fact of the sensitivity of nuclear stopping towards isospin content of in-medium nucleon-nucleon cross-section above Fermi energy. In the recent study on in-medium elastic nucleon-nucleon cross-section using the energy isotropy ratio for protons only. It was found that the NN cross-section is significantly reduced as compared to the corresponding vacuum value and this reduction is composed of the Pauli blocking factor and the in-medium quenching (η) factors [14]. Furthermore, we have various studies that mentioned the significance of in-medium effects and reduction of NN cross-section. The parametrized form of in-medium NN cross-sections in our dynamical model is $\sigma_{\rm NN}^{\rm med} = F\sigma_{\rm NN}^{\rm free}$ where F is the correction factor for in-medium effects.

In the present study, we shall try to investigate various observables of nuclear stopping. We simulated various reactions, i.e. ^{40}Ca+^{40}Ca, ^{58}Ni+^{58}Ni,

^{129}Xe+^{120,124}Sn and ^{197}Au+^{197}Au for central collisions. We aim to shed light on the observables like energy-based isotropy ratio (R_E), momentum-based isotropy ratio (R_P), and the ratio of variances of the transverse to longitudinal rapidity distribution (*vartl*) corresponding to energy dependence for soft momentum dependent equation of state using IQMD model. Eventually, we will try to extract information about the form of the correction factor (F) in the NN cross-section by comparing our IQMD results with the available set of experimental data of nuclear stopping from tens of MeV/nucleon to thousands of MeV/nucleon. The earlier studies available are only in a restricted-energy domain. Furthermore, for the assertion, we will also study the isospin tracing method to take care of the in-medium effect in the reduction factor of the NN cross-section using different combination reactions of ^{96}Zr+^{96}Ru and ^{96}Ru+^{96}Zr.

2 The Model

The Isospin-dependent Quantum Molecular Dynamics (IQMD) model [15] is an N-body approach simulating heavy-ion reactions at intermediate energies on an event-by-event basis. In this model, nucleons are represented by Gaussian-shaped density distributions and Wigner distribution function f_i of i-th nucleon is expressed as:

$$f_i(\vec{r},\vec{p},t) = \frac{1}{\pi^3\hbar^3}\exp\Big(-[\vec{r}-\vec{r_i}(t)]^2\frac{2}{L}\Big)\times\exp\Big(-[\vec{p}-\vec{p_i}(t)]^2\frac{L}{2\hbar^2}\Big). \quad (1)$$

where ($\vec{r}$, $\vec{p}$) is the phase space position of nucleon in the centre of mass of collision. Nucleons are initialized in a sphere with radius $R = 1.12A^{1/3}$ fm, in accordance with the liquid-drop model corresponding to a ground state density of $\rho_0 = 0.17$ fm^{-3}, which results in Fermi momentum ($\vec{p_F}$) of 268 MeV/c. The initial momenta of nucleons are randomly chosen between 0 and Fermi momentum. The nucleons of the target and projectile interact by two-body and three-body Skyrme forces, Yukawa potential, Coulomb interactions, symmetry potential, and momentum-dependent interactions. The hadrons propagate using the Hamilton equations of motion:

$$\frac{d\vec{r_i}}{dt} = \frac{d\langle H\rangle}{d\vec{p_i}}; \qquad \frac{d\vec{p_i}}{dt} = -\frac{d\langle H\rangle}{d\vec{r_i}} \quad (2)$$

with

$$\begin{aligned}\langle H\rangle &= \langle T\rangle + \langle V\rangle \\ &= \sum_i \frac{p_i^2}{2m_i} + \sum_i\sum_{j>i}\int f_i(\vec{r},\vec{p},t)V_{ij}(\vec{r}',\vec{r})f_j(\vec{r}',\vec{p}',t)d\vec{r}d\vec{r}'d\vec{p}d\vec{p}'\,. \quad (3)\end{aligned}$$

As stated above, the baryon potential V_{ij}, consists of the Coulomb interaction between the charged particles, Skyrme-type interaction, Yukawa potential,

momentum-dependent part (iso-scalar), and symmetry potential. All these interactions are well defined in the Ref. [15]. The nuclear symmetry energy used is proportional to density and two forms of NN cross-section are used ; one where $\sigma_{\rm NN}^{\rm med} = \sigma_{\rm NN}^{\rm free}$ (i.e. no in-medium effects) and second; $\sigma_{\rm NN}^{\rm med} = F\sigma_{\rm NN}^{\rm free}$ [and F is the correction factor to mimic the in-medium effects] [16]. Note that a reduction of 20% [$F = 0.8$] NN cross-section due to in-medium effects is advocated by the previous studies carried out using same IQMD approach where investigation of transverse flow and its disappearance (around Fermi energy range) are done and an excellent agreement with measurements is reported for the above form of reduction factor [16]. However, here, the energy range spans a wider values from tens of MeV/nucleon to GeV/nucleon and thus it is expected that a constant reduction factor throughout the energy range is not sufficient. Note that energy-dependent correction factor is also with $F = 0.8$ motivated by other recent studies [17,18]. Keeping in view all these, we have done the calculations for 20% reduction effects in NN cross-sections. Further, details about these cross-sections for proton-proton (or neutron-neutron) and proton-neutron collisions can be found in [15, 19]. The cross-sections for neutron-neutron collisions are assumed to be equal to the proton-proton cross-sections. Two particles collide if their minimum distance *d* fulfills

$$d \leq d_0 = \sqrt{\frac{\sigma_{\rm tot}}{\pi}}, \qquad \sigma_{\rm tot} = \sigma(\sqrt{s}, \text{type}), \tag{4}$$

where 'type' denotes the ongoing collision partners. Explicit Pauli blocking is also included; i.e. Pauli blocking of neutrons and protons is treated separately. This transport approach (primary model) generates phase space of nucleons and to identify cluster/fragment, the minimum spanning tree (MST) method is utilized (as a secondary model). This approach is based on spatial constraints among nucleons and two nucleons are thought to be a part of the same cluster/fragment if they are separated by (at maximum) 2.8 fm, i.e. $(r_i - r_j) \leq 2.8$ fm. Note that MST method works well to depict the correct fragmentation pattern at the final stages of heavy-ion collisions [20,21].

3 Results and Discussion

The observables of nuclear stopping which we studied are:

(1) Energy-based isotropy ratio (R_E) [8] and is defined as the ratio of transverse energy to parallel energy and given as,

$$R_E = \frac{\sum E_\perp}{2\sum E_\parallel}, \tag{5}$$

where $E_\perp$ ($E_\parallel$) is the transverse (parallel) energy of emitted particles in the center of the mass frame and the sum runs over all the particle's size.

(2) Momentum-based isotropy ratio R_p [8], which is defined as the ratio of transverse to parallel momenta of produced particles and given as,

$$R_p = \frac{2}{\pi}\frac{\sum p_\perp}{\sum p_\parallel}, \tag{6}$$

where $p_\perp$ ($p_\parallel$) is the transverse (parallel) momenta in the center of the mass system and the sum runs over all the particle's size.

(3) Ratio of variances of the transverse to longitudinal rapidity distribution [9] and given as,

$$vartl = \frac{\sigma(y_\perp)}{\sigma(y_\parallel)}, \tag{7}$$

where $\sigma(y_\perp)$ and $\sigma(y_\parallel)$ are the variances of rapidity distribution of particles in transverse and longitudinal direction.

(4) Another observable to further verify the incomplete stopping in HIC is the so-called iso-spin tracing [22]. It helps to identify the relative yield of the particles by examining their isospin content in a given region of momentum phase space. And for this, we are using 2 different isobars (^{96}Ru+^{96}Zr and ^{96}Zr+^{96}Ru), exchanging target and projectile roles between them, and lastly comparing it with the collisions of an identical system (^{96}Zr+^{96}Zr and ^{96}Ru+^{96}Ru). Iso-spin tracing is given by [22]

$$R_Z = \frac{2N_y^{\rm mix} - N_y^{\rm Zr} - N_y^{\rm Ru}}{N_y^{\rm Zr} - N_y^{\rm Ru}} \tag{8}$$

where N_y is an isospin sensitive observable at rapidity (y) *viz.* yield of protons or $t/^3$He ratios. Note that $N_y^{\rm Zr}$ ($N_y^{\rm Ru}$) is the value obtained for ^{96}Zr+^{96}Zr (^{96}Ru+^{96}Ru) collisions and $N_y^{\rm mix}$ is the value observed for ^{96}Zr+^{96}Ru or ^{96}Ru+^{96}Zr collisions. R_Z can take values +1 and -1 for target-target collisions and projectile-projectile collisions.

In Figure 1, we calculate the evolution of R_E for collisions of ^{58}Ni+^{58}Ni, ^{129}Xe+^{120,124}Sn, and ^{197}Au+^{197}Au as a function of incident energy for protons only at central collisions ($b < 0.14$ fm), where solid square represents the full NN cross-section (FCS) ($\sigma_{\rm NN}^{\rm free}$) calculation while the open square represents the 20% reduction (RCS) in NN cross-section, i.e. $\sigma_{\rm NN}^{\rm med} = 0.8\sigma_{\rm NN}^{\rm free}$ and stars represent the experimental data [13]. From Figure 1, it is seen that the decreasing trend of R_E as a function of incident energy up to Fermi energy. This is because of mean field dominance at this energy range over NN collisions in the HIC process [23]. Above Fermi energy, NN collisions start dominating over the mean field and due to this dominance of NN collisions, initial longitudinal momenta of protons start to transform into transverse momenta, and therefore, R_E starts increasing as shown in Figure 1. From Figure 1, it is also seen that value of R_E is more for higher mass system (i.e. the value of R_E is more for ^{197}Au+^{197}Au than ^{129}Xe+^{120,124}Sn and ^{58}Ni+^{58}Ni) for same incident energy range which

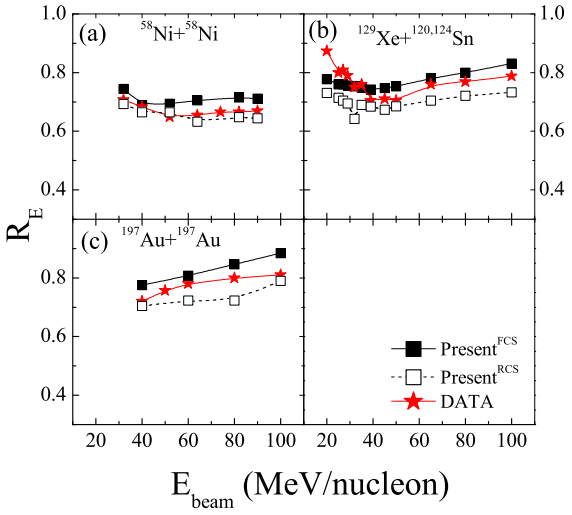

Figure 1. Isotropy ratio (R_E) for central ($0 \leq \hat{b} \leq 0.14$) collisions of ^{58}Ni+^{58}Ni (a), ^{129}Xe+^{120,124}Sn (b) and, ^{197}Au+^{197}Au (c) as a function of incident energy. Calculations are represented by closed and open symbols and experimental measurements are shown by stars [13]. Various symbols are explained in text. Lines are only to guide the eye.

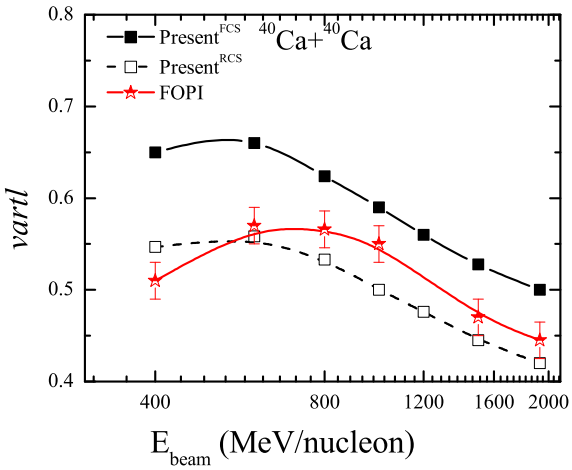

Figure 2. Excitation function of the nuclear stopping observable *vartl* for central collisions ^{40}Ca+^{40}Ca as a function of incident energy. Experimental data [9] is shown by stars and calculations are displayed by closed and open symbols and various lines. Symbols are explained in text.

indicates that nuclear stopping is related to the number of participants in the system and this result is supported by the previous study of Glauber description of collisions [24]. In the comparison of our calculations with experimental data, it is seen that the open square has better agreement with the measured value of R_E for protons only. From the above analysis, we may conclude that it is necessary to reduce the in-medium NN reduction to around 20% to study the nuclear stopping observable for soft-momentum dependent (SMD) EOS for the incident energy range from 10–100 MeV/nucleon using a dynamical model.

In Figure 2, we studied *vartl*, which is also an important observable of nuclear stopping. We calculate the *vartl* as a function of incident energy of range 400 MeV/nucleon to 1930 MeV/nucleon for SMD EOS using the IQMD model for collisions of Ca+Ca and for impact parameter $b < .15$, where symbols have the same meaning as defined in Figure 1. In the previous study of *vartl*, it is noted that the value of *vartl* firstly increases with incident energy and then reaches a plateau between 200 MeV/nucleon and 800 MeV/nucleon and then start decreases at higher incident energies. From Figure 2, it is seen that the fast drop of the value of *vartl* as a function of incident energy, is because of the production of delta resonances and pions at higher incident energy to the in-elastic channel in the NN cross-section. On comparing our calculations with measured values of *vartl* for incident energy [9], it may be concluded that to study the nuclear

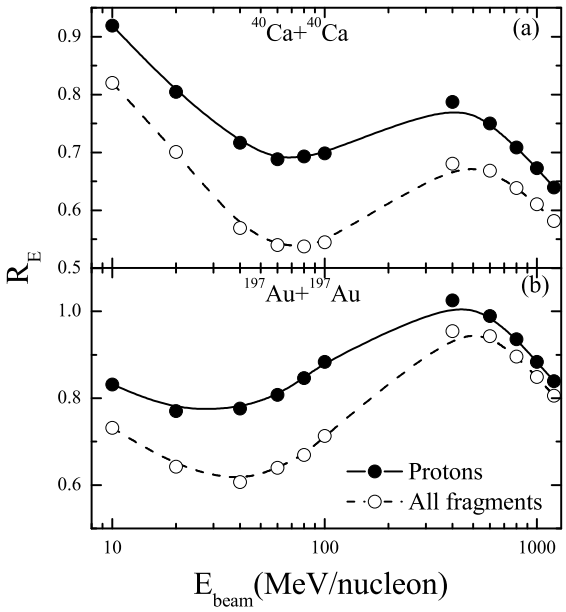

Figure 3. Isotropy ratio R_E for ^{40}Ca+^{40}Ca and ^{197}Au+^{197}Au collisions at 60 MeV/nucleon and 400 MeV/nucleon as a function of beam energy.

stopping observables with the help of a dynamical model, the in-medium NN cross-section must be reduced around 10% to 20% at higher incident energies.

To strengthen our interpretation of the results, we investigate the R_E as a function of incident energy (10–1000 MeV/nucleon) for collisions of ^{40}Ca+^{40}Ca and ^{197}Au+^{197}Au as shown in Figure 3. Here, the dark circle and open circle represent the ^{40}Ca+^{40}Ca and ^{197}Au+^{197}Au for protons only and all nucleons respectively, for impact parameter $b < .14$ fm. From Figure 3, it is seen that the high value of R_E at low incident energy starts decreasing till the Fermi energy range because of the mean-field dominance over NN collisions, and again the value of R_E starts to increase with increasing incident energy, this is because the role of the mean-field is suppressed by NN collisions while at higher incident energies, the value of R_E sharply decreases this is because of production of delta resonances and pions as shown in Figure 3. Higher value of R_E for protons than all nucleons is because of the fact that the protons have emerged from a thermalized source. we also investigated the R_E for lighter systems, i.e. ^{40}Ca+^{40}Ca. Similar behavior for R_E is found but the value of R_E is a small comparison to ^{197}Au+^{197}Au and this is because R_E is related to the number of participants in the system. A similar type of study is observed in Ref. [25] where central collisions of ^{58}Ni+^{58}Ni and ^{129}Xn+^{124}Sn are investigated.

Another observable to see the incomplete stopping of HIC is the isospin tracing method [22]. Figure 4 represents the isospin mixing (R_Z) as a func-

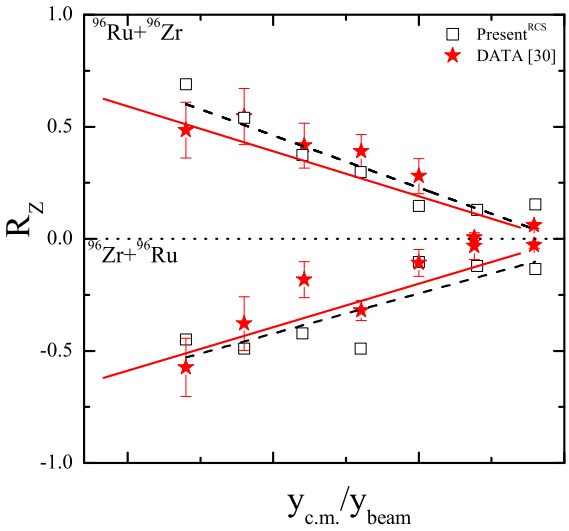

Figure 4. Isospin tracer observable R_Z for protons in central collisions of ^{96}Zr+^{96}Ru and ^{96}Ru+^{96}Zr at incident energy of 400 MeV/nucleon. Our calculations are represented by sqaures and stars represent experimetal data [22]. Solid lines are linear fit of data. Different lines are explained in text and stars represent experimental measurements.

tion of rapidity distribution along with experimental results (represent by the stars) [22] for reactions of ^{96}Zr+^{96}Ru and ^{96}Ru+^{96}Zr at an incident energy of 400 MeV/nucleon and impact parameter $b < 1.0$. The open square represents the calculated values of ^{96}Ru+^{96}Zr and ^{96}Zr+^{96}Ru for SMD EOS with a 20% reduction in NN cross-section by using IQMD model. From equation (3), it is concluded that the value of $R_Z = 1$(-1), when the momentum phase space is filled with protons originated from Zr(Ru) nucleus and therefore complete stopping is defined as the complete mixing of the protons which are equally arising from Zr as well as Ru. The value of the full stopping is expected to be a yield of $R_Z = 0$. The slope is 0.3568 and -0.4659 for 20% reduction in NN cross-section and 0.223 and -0.56206 for full NN cross-section for collisions of ^{96}Zr+^{96}Ru and ^{96}Ru+^{96}Zr and 0.39 and -0.39 for experimentally measured slopes of reactions ^{96}Zr+^{96}Ru and ^{96}Ru+^{96}Zr [22]. In the comparison of the experimental data with our calculation, it is found that 20% reduction of NN cross-section for SMD EOS has better agreement with experimental data.

4 Summary

We have studied various nuclear stopping observables for collisions of ^{40}Ca+^{40}Ca, ^{58}Ni+^{58}Ni, ^{129}Xe+^{120,124}Sn, and ^{197}Au+^{197}Au as a function of incident energy range from tens of MeV/nucleon to GeVs/nucleon for soft momentum dependent equation of state using IQMD model. In the comparison of our calculations with experimental data, it is found that: (a) 20% reduction in in-medium NN cross-section is necessary for study energy Isotropy ratio (R_E) in the Fermi energy range; (b) around 20% reduction in in-medium NN cross-section is favorable in the study of *vartl* at higher incident energy for the reactions of ^{40}Ca+^{40}Ca; (c) Isospin mixing (R_Z) also has good agreement with 20% in-medium reduction.

References

[1] S. Gautam, *Phys. Rev.* C **83** (2011) 064604.

[2] H. Stocker, W. Greiner, *Phys. Rep.* **137** (1986) 277;
P. Danielewicz, R. Lacey, W.G. Lynch, *Science* **298** (2002) 1592;
T. Klahn, et al., *Phys. Rev. C* **74** (2006) 035802 (2006).

[3] J.M. Lattimer, M. Prakash, *Astrophys. J.* **550** (2001) 426.

[4] J. Aichelin, *Phys. Rep.* **202** (1991) 233;
C. Hartnack, et al., *Eur. Phys. J. A* **1** (1998) 151;
E.E. Kolomeitsev, et al., *J. Phys. G* **31** (2005) s741 (2005).

[5] C.Y. Wong, *Introduction to High-Energy Heavy-Ion Collisions* (World Scientific, Singapore, 1994).

[6] B.A. Li, C.M. Ko, *Nucl. Phys. A* **601** (1996) 457.

[7] W. Bauer, *Phys. Rev. Lett.* **61** (1988) 2534.

[8] G. Lehaut, et al., *Phys. Rev. Lett.* **104** (2010) 232701.

[9] W. Reisdorf, et al., *Phys. Rev. Lett.* **92** (2004) 232301.

[10] R. Rana, S. Gautam, R.K. Puri *Nucl. Phys. A* **1016** (2021) 122324.

[11] S. Kumar, S. Kumar, R.K. Puri, *Phys. Rev. C* **81** (2010) 014601.
[12] C. Hartnack, *Phys. Rev. Lett.* **96** (2006) 012302.
[13] M. Henri, et al., *Phys. Rev. C* **101** (2020) 064622.
[14] L. Ou, X. He, *Chin. Phys. C* **43** (2019) 044103.
[15] C. Hartnack, R.K. Puri, J. Aichelin, J. Konopka, S.A. Bass, H. Stocker, W. Greiner, *Eur. Phys. J. A* **1** (1998) 151.
[16] S. Gautam, et al., *J. Phys G: Nucl. Part. Phys.* **37** (2012) 085102.
[17] P. Li, et al., *Phys. Rev. C* **97** (2018) 044620.
[18] Q.F. Li, et al., *Phys. Rev. C* **83** (2011) 044617.
[19] B.J. Verwest, R.A. Arndt, *Phys. Rev. C* **25** (1982) 1979;
S.A. Bass, et al., *Phys. Rev. C* **51** (1994) 3343.
[20] J. Aichelin, *Phys. Rep.* **202** (1991) 233.
[21] R. Kumar, S. Gautam, R.K. Puri, *Phys. Rev. C* **89** (2014) 064608.
[22] F. Rami, et al., *Phys. Rev. Lett.* **84** (2000) 1192.
[23] P. Lautesse, et al., *Eur. Phys. J. A* **27** (2006) 349.
[24] S.K. Charagi, S.K. Gupta, *Phys. Rev. C* **41** (1990) 1610.
[25] G.Q. Zhang, et al., *Phys. Rev. C* **84** (2011) 034612.